$Sr_8MgSc(PO_4)_7:Eu^{2+}$ Phosphor: d – f Transition Driven Applications for Solid-State Lighting and Extreme Environment Multimode Sensing Inspections

Table S1. Ionic radii of Sr^{2+} and Eu^{2+} in different coordination environments.

Ion	Coordination	Ionic Radius (Å)
Sr^{2+}	VI	1.18
	VII	1.21
	VIII	1.26
	IX	1.31
	X	1.36
Eu^{2+}	VI	1.17
	VII	1.20
	VIII	1.25
	IX	1.30
	X	1.35

Table S2. Quantum efficiency of SMSP:x% Eu^{2+} (x = 0.025 – 1) phosphors

Sample	η_{IQE} (%)	η_{EQE} (%)
SMSP:0.025Eu^{2+}	17.9%	9.8%
SMSP:0.05Eu^{2+}	25.67%	14.7%
SMSP:0.1Eu^{2+}	29.64%	18.1%
SMSP:0.2Eu^{2+}	31.27%	19.6%
SMSP:0.5Eu^{2+}	21.45%	12.3%
SMSP:1Eu^{2+}	15.85%	8.9%

Table S3. Bond length of the Sr1-O for the SMSP:0.2% Eu^{2+} and SMSP host samples.

	SMSP host	SMSP:0.2% Eu^{2+}
Sr1-O1	3.10771(1)	3.33724(1)
Sr1-O3	3.29204(2)	3.19379(8)
Sr1-O7	3.06274(2)	2.81341(1)
Sr1-O8	2.77284(1)	2.74760(1)
Sr1-O9	2.47385(1)	2.55908(7)
Sr1-O12	2.51631(1)	2.92903(6)
Sr1-O13	2.65096(1)	2.31305(7)
Sr1-O14	2.89014(7)	2.71916(6)
Average Sr1-O	2.84672	2.82651

Table S4. Bond length of the Sr2-O for the SMSP:0.2% Eu^{2+} and SMSP host samples.

	SMSP host	SMSP:0.2% Eu^{2+}
Sr2-O2	2.74370(1)	2.76115(1)
Sr2-O4	2.54253(1)	2.71409(9)
Sr2-O5	2.94653(1)	2.75710(1)
Sr2-O6	2.53527(1)	2.77373(8)
Sr2-O10	2.53808(1)	2.58961(7)
Sr2-O12	2.54356(9)	2.44142(7)
Sr2-O13	2.35415(1)	2.58378(1)
Sr2-O14	2.71012(6)	2.88999(9)
Average Sr2-O	2.61493	2.68892

Table S5. Bond length of the Sr3-O for the SMSP:0.2% Eu^{2+} and SMSP host samples.

	SMSP host	SMSP:0.2% Eu^{2+}
Sr3-O1	2.67841(3)	3.25581(9)
Sr3-O2	3.32560(5)	3.08125(9)
Sr3-O5	3.08651(8)	3.27481(9)
Sr3-O6	2.82945(6)	2.33764(8)
Sr3-O7	2.60307(6)	2.49114(8)
Sr3-O9	2.53353(2)	2.71164(5)
Sr3-O11	2.40011(7)	2.52803(7)
Average Sr3-O	2.77961	2.81150

Table S6. Bond length of the Sr5-O for the SMSP:0.2% Eu^{2+} and SMSP host samples.

	SMSP host	SMSP:0.2% Eu^{2+}
Sr5-O1	2.48860(8)	2.62239(7)
Sr5-O3	2.63180(1)	2.63960(1)
Sr5-O3	2.82673(4)	2.98858(3)
Sr5-O4	2.71201(2)	2.63836(4)
Sr5-O7	2.41515(9)	2.31262(1)
Sr5-O11	2.51298(6)	2.47610(2)
Sr5-O13	2.68101(6)	2.72184(8)
Average Sr5-O	2.60983	2.62850

Table S7. Comparison of luminescence thermal stability of different phosphors

Sample	λ_{ex} (nm)	$I_{373\ K}/I_{298\ K}$ (%)	Reference
SMSP: Eu^{2+}	342	50.01	This work
$Sr_9LiMg(PO_4)_7:Eu^{2+}$	405	27	[1]
$Sr_9Sc(PO_4)_7:Eu^{2+}$	360	30	[2]
$Ba_3Si_6O_{15}:Eu^{2+}$	360	26	[3]

Table S8. The optical properties of WLED devices have been reported.

Samples	CIE (x, y)	CCT (K)	Ra	references
SMSP:0.2% Eu^{2+}	(0.3509, 0.3397)	4718 K	93.2	This work
$Ba_3GdNa(PO_4)_3F:Eu^{2+}$	(0.273, 0.275)	5402 K	81	[4]
$Ba_2Ca(PO_4)_{1.6}(BO_3)_{0.4}:Eu^{2+}$	—	6488 K	90.4	[5]
$K_2BaCa(PO_4)_2:Eu^{2+}, Mn^{2+}$	(0.298, 0.383)	6789 K	74.7	[6]

Table S9. Comparison of dλ / dp and red shift values of different rare earth doped phosphors under high pressure

Sample	λ_{ex} (nm)	dλ / dp	Red shift (nm)	Ref
SMSP:Eu^{2+}	342	2.03	42	This work
$BaLi_2Al_2Si_2N_6$: Eu^{2+}	400	1.5813	35	[7]
$Mg_2Gd_8(SiO_4)_6O_2:Ce^{3+}$	490	1.8453	60	[8]
$Lu_2Mg_2Al_2Si_2O_{12}$: Eu^{2+}	355	1.68	19	[9]

Table S10. Comparison of pressure sensing sensitivity of different rare earth doped phosphors

Materials	Pressure	S_{pa}(GPa^{-1})	S_{pr}(% GPa^{-1})	Ref.
SMSP:Eu^{2+}	0 – 21.5 GPa	0.96	21.8	this work
$Lu_2Mg_2Al_2Si_2O_{12}:Eu^{2+}, Mn^{2+}$	0 – 25.6 GPa	0.0494	1.89	[10]
$SrB_4O_7:Eu^{2+}/Sm^{2+}$	10 – 40 GPa	0.35	13.8	[11]
$Li_4SrCa(SiO_4)_2:Eu^{2+}$	0 – 15.7 GPa	0.299	9.9	[12]

Table S11. Comparison of pressure dynamic sensitivity of different phosphors

Materials	Pressure	S_{pr}(% GPa^{-1})	Ref.
SMSP:Eu^{2+}	0 – 21.5 GPa	116.22	this work
$LiScGeO_4$:Cr^{3+}	0 – 9.78 GPa	121.14	[13]
$Li_2Mg_3TiO_6$:Cr^{3+}	0 – 10.05 GPa	4.7	[14]
MgO:Cr^{3+}	0 – 8 GPa	9.83	[15]

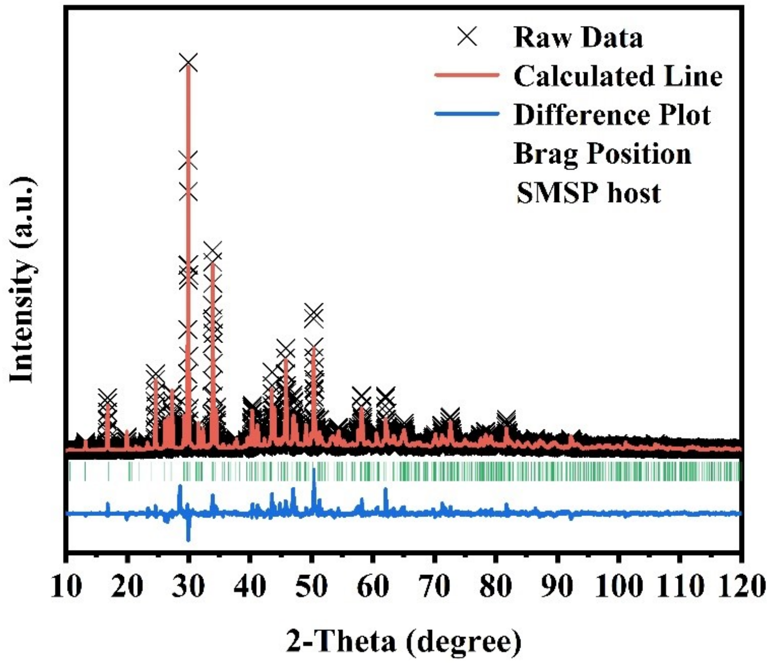

Fig. S1 Rietveld analysis patterns for XRD data of the SMSP host.

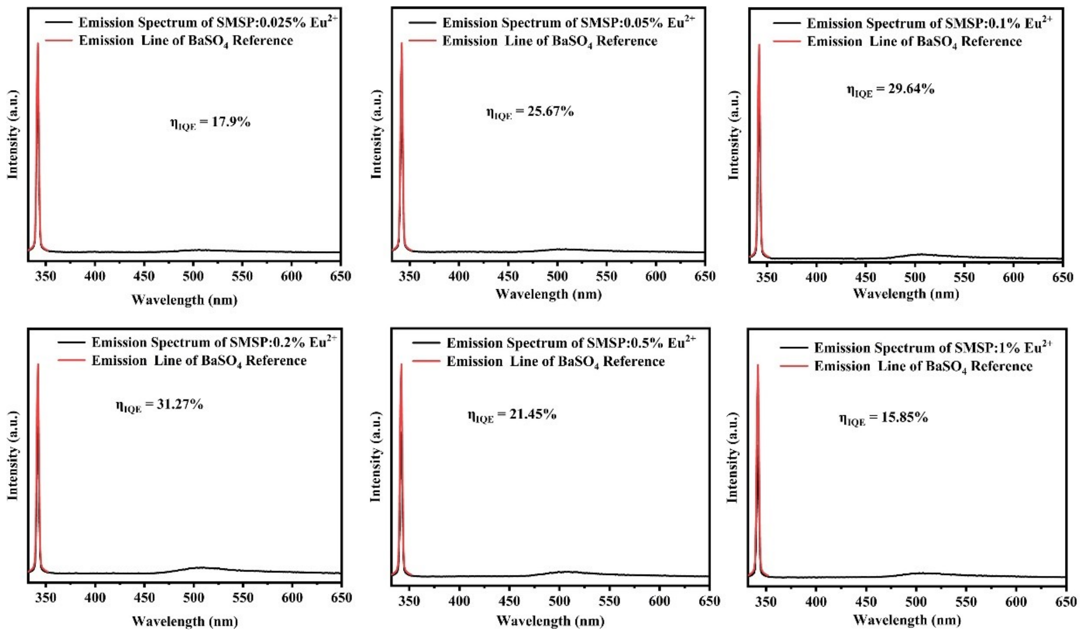

Fig. S2 Quantum efficiency of SMSP:x% Eu^{2+} (x = 0.025 – 1) phosphors

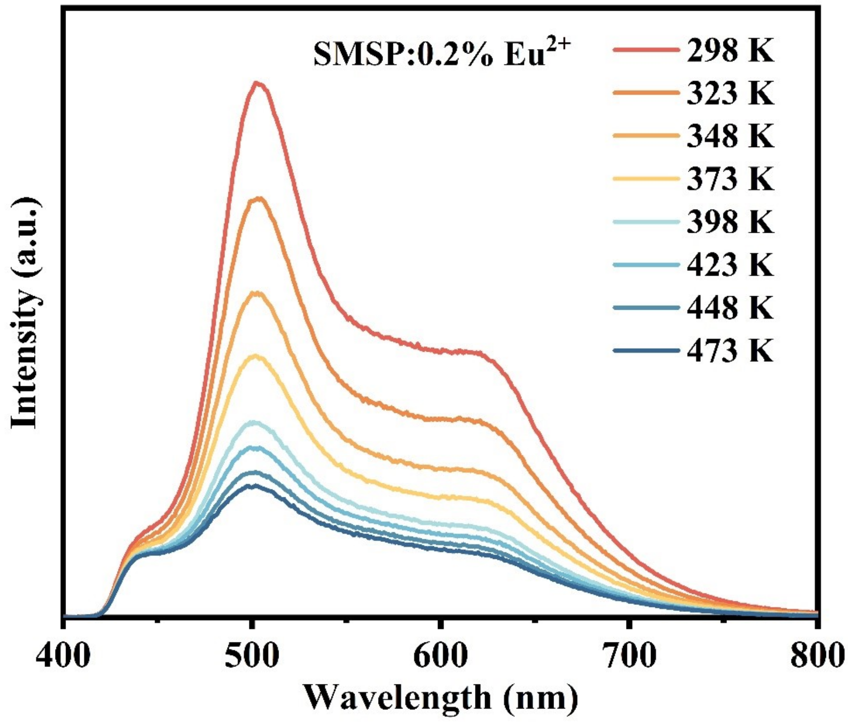

Fig. S3 PL spectra of SMSP:0.2% Eu^{2+} at 298K-473K temperature

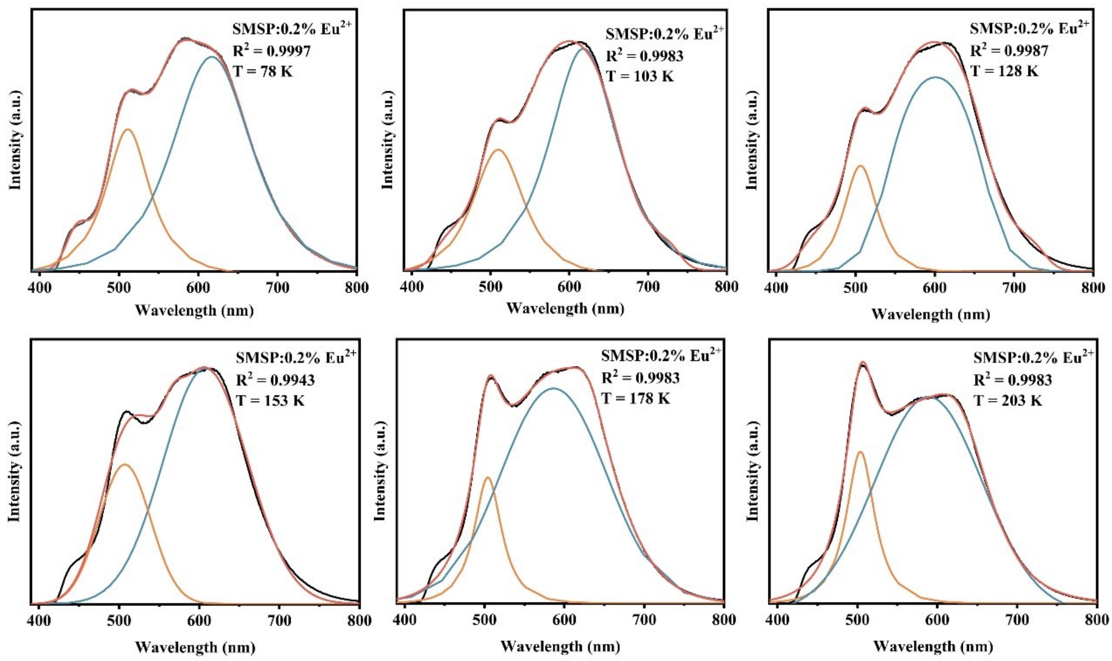

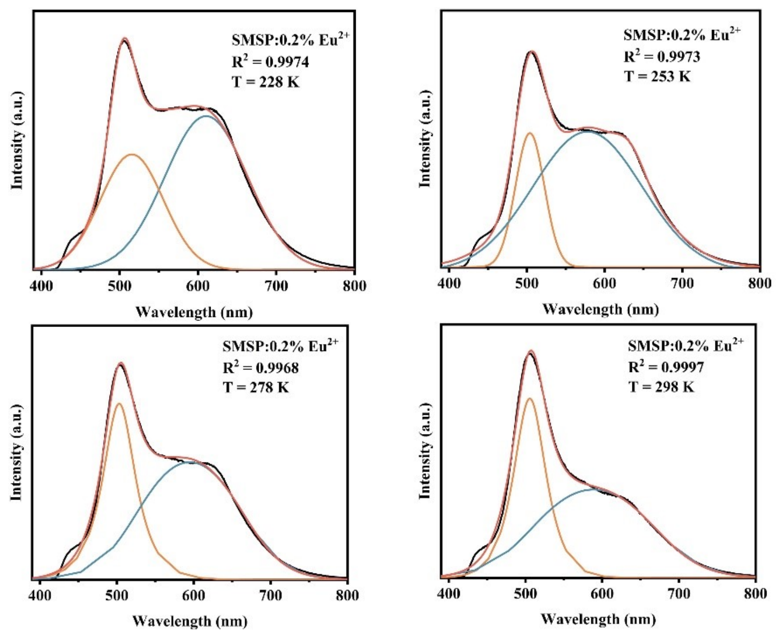

Fig. S4 Gaussian fitting diagrams of two position of SMSP:0.2% Eu^{2+} under different temperature (289 K → 78 K)

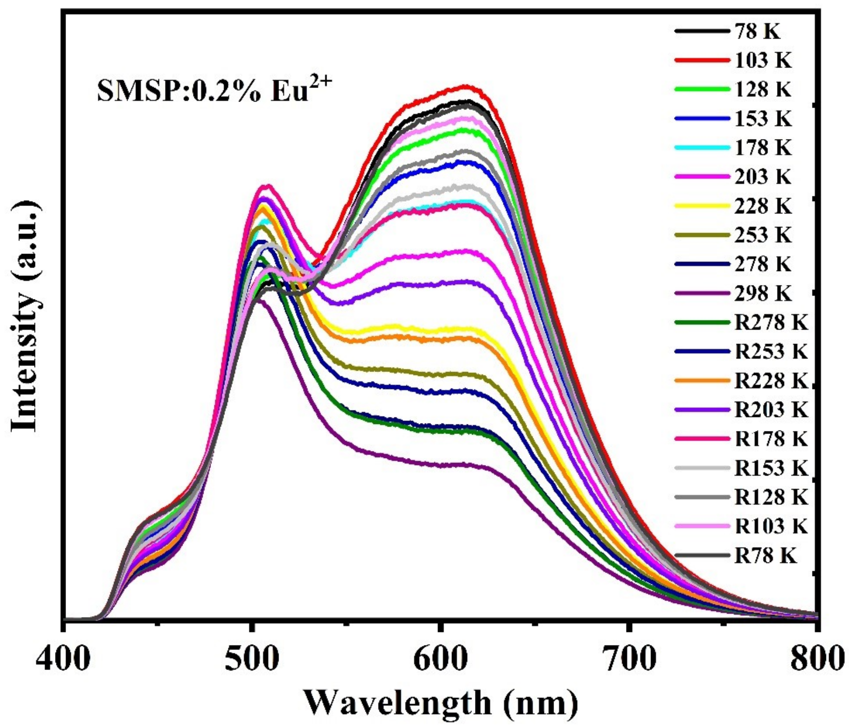

Fig. S5 PL spectra of SMSP:0.2% Eu^{2+} at 298K-78K-298K temperature

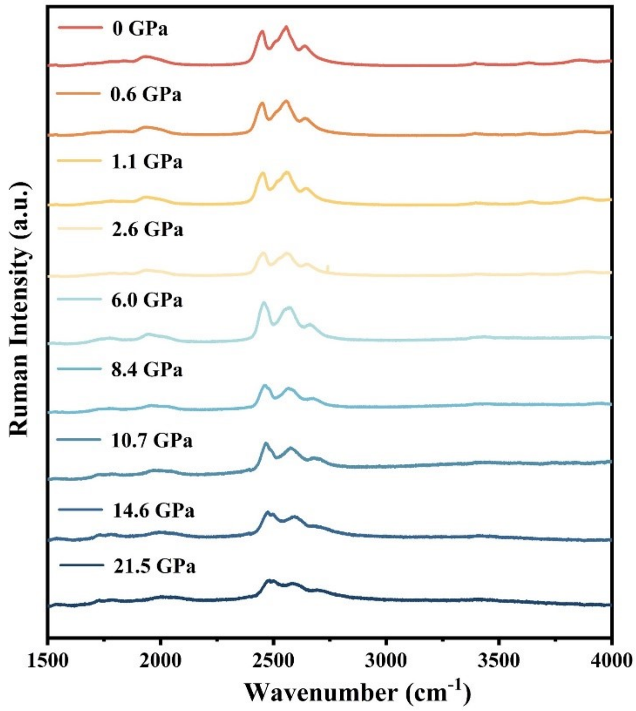

Fig. S6 Raman spectra of the SMSP:0.2% Eu^{2+} sample at different pressures

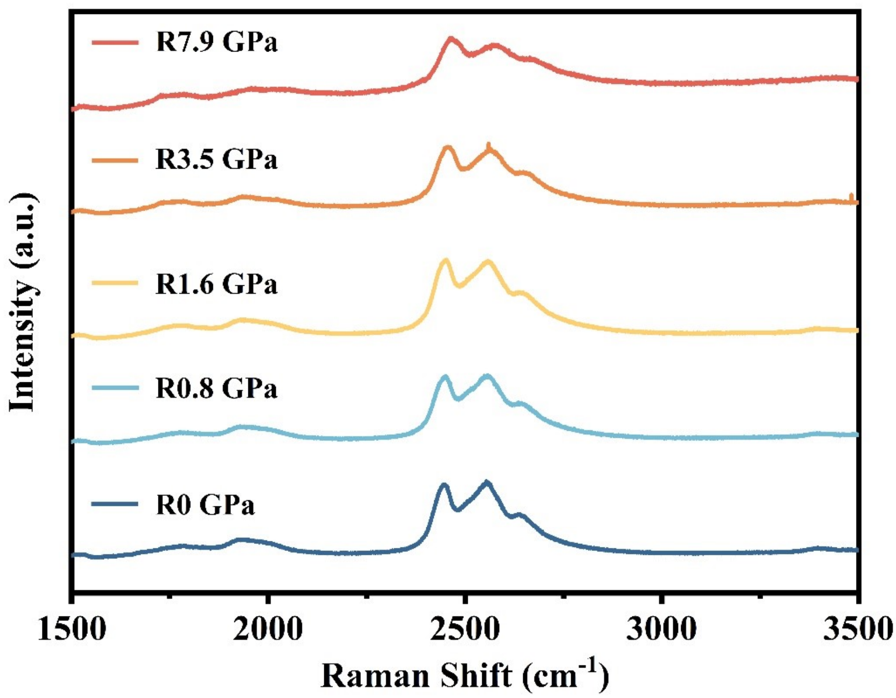

Fig. S7 Raman spectra of the SMSP:0.2% Eu^{2+} sample during decompression.

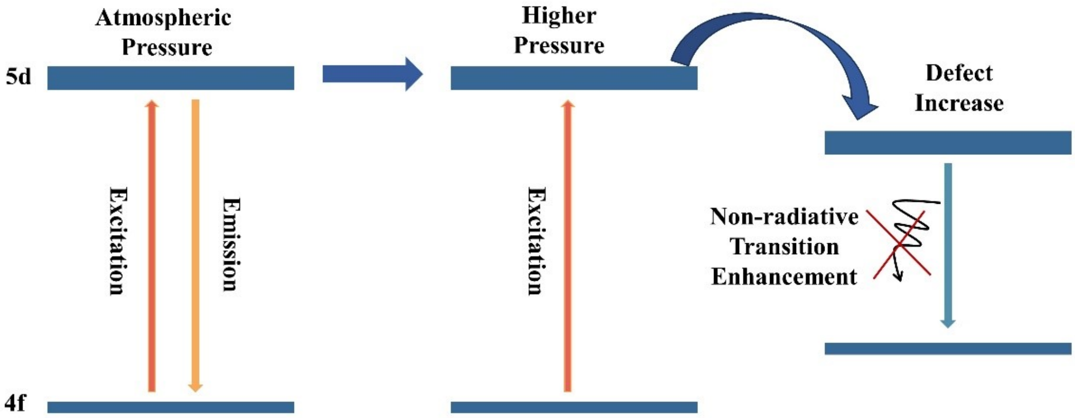

Fig. S8 Schematic diagram of the influence of defects on the intensity

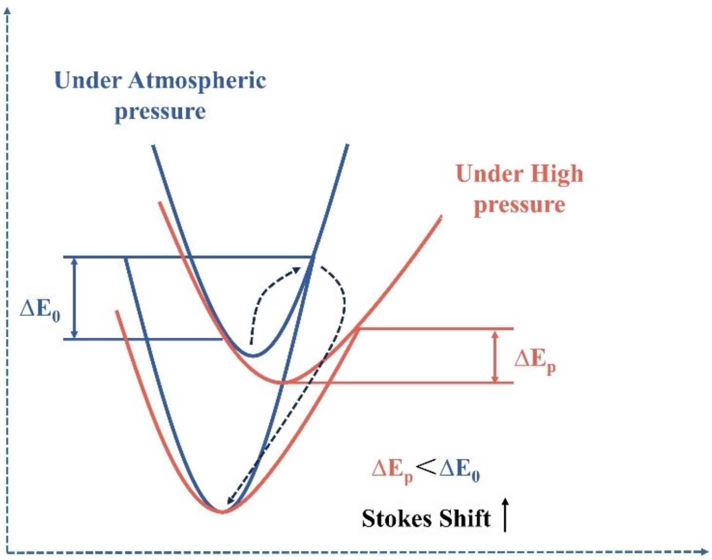

Fig. S9 Schematic illustration of the nonradiative transition.

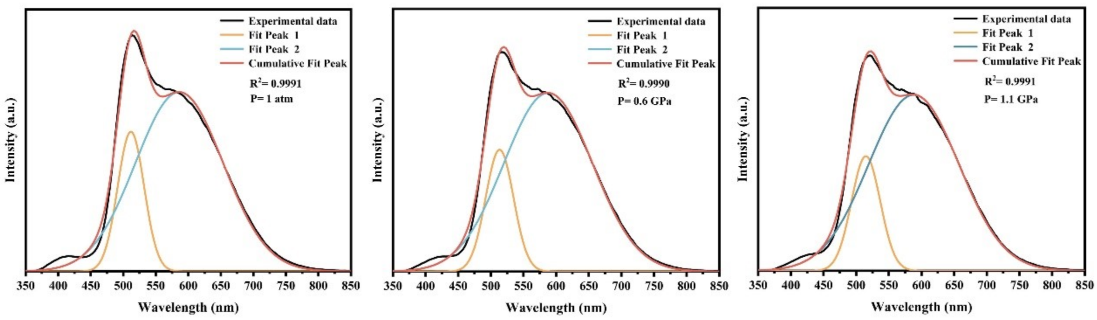

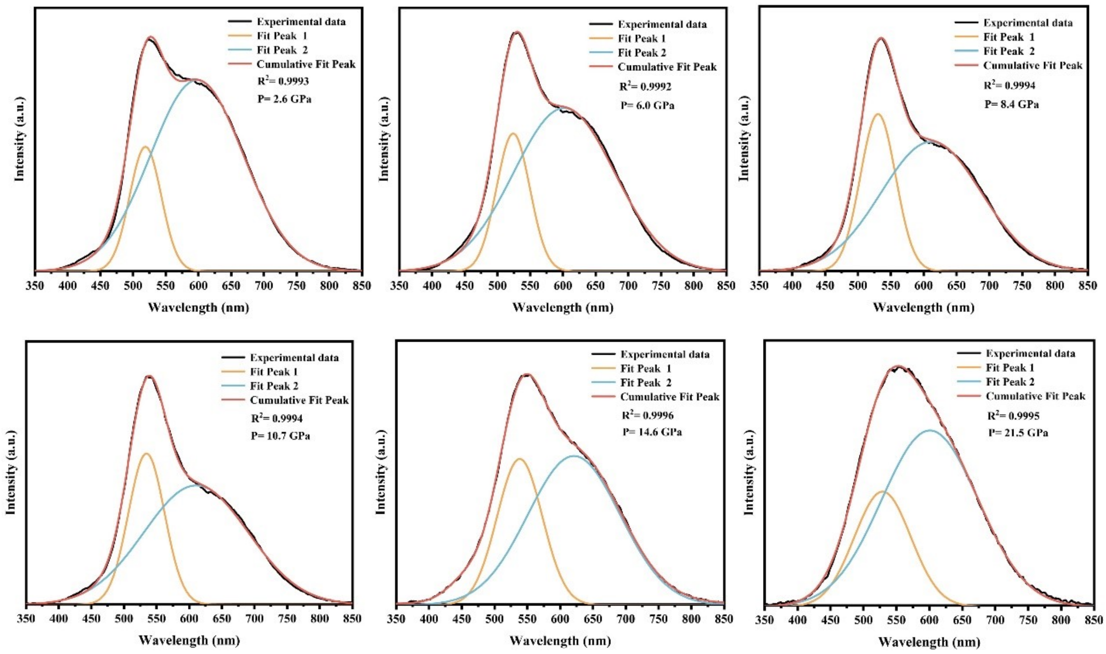

Fig. S10 Gaussian fitting diagrams of two positions of SMSP:0.2% Eu^{2+} under different pressures

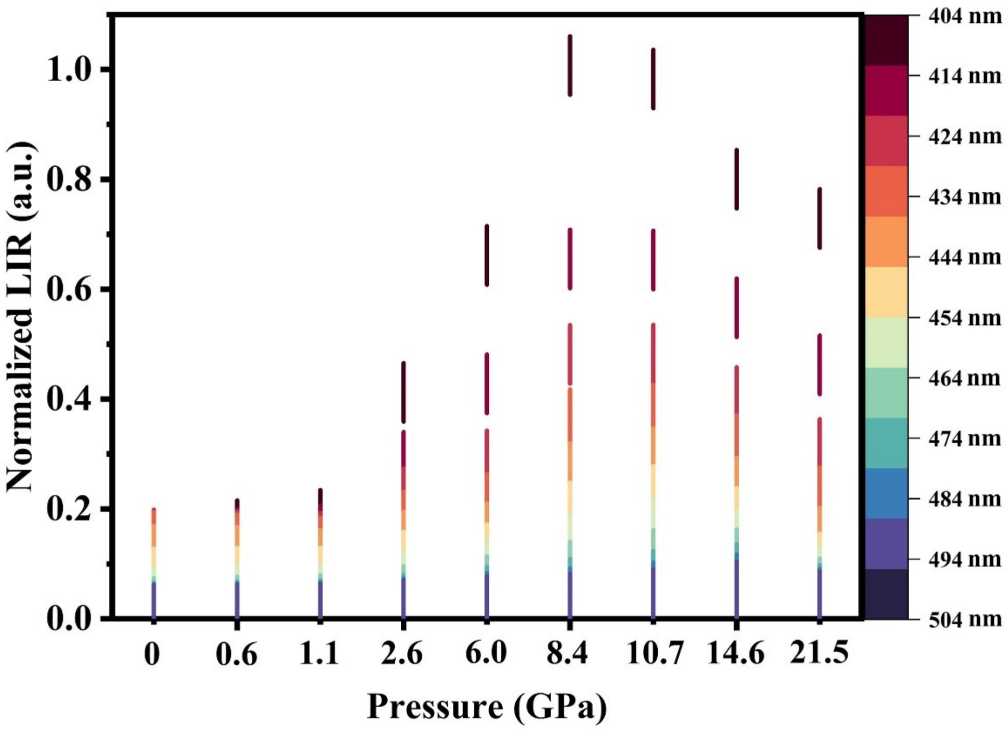

Fig. S11 The LIR as a function of pressure.

$$LIR = 0.038 - 0.046p + 0.029p^2 - 7.6 \times 10^{-3}p^3 + 9.8 \times 10^{-4}p^4 - 4.8 \times 10^{-5}p^5$$

(F1)

Quantum efficiency calculation formula:[16]

$$\eta_{IQE} = \frac{\varepsilon}{\alpha} = \frac{\int L_S}{\int E_R - \int E_S} \quad \text{(F2)}$$

$$\alpha_{abs} = \frac{\alpha}{\delta} = \frac{\int E_R - \int E_S}{\int E_R} \quad \text{(F3)}$$

$$\eta_{EQE} = \frac{\varepsilon}{\delta} = \frac{\int L_S}{\int E_R} \quad \text{(F4)}$$

References

1. X. Ding, Y. Wang, Novel Orange Light Emitting Phosphor Sr_9(Li, Na, K)$Mg(PO_4)_7$: Eu^{2+} Excited by NUV Light for White LEDs, Acta Materialia, 2016, **120**, 281-291.
2. D. Kim, Y.W. Seo, S.H. Park, B.C. Choi, J.H. Kim, J.H. Jeong, Theoretical Design and Characterization of High Efficient $Sr_9Ln(PO_4)_7$: Eu^{2+} Phosphors, *Mater Res Bull*, 2020, **127**, 110856.
3. M. Shang, S. Liang, N. Qu, H. Lian, J. Lin, Influence of Anion/Cation Substitution ($Sr^{2+} \rightarrow Ba^{2+}$, $Al^{3+} \rightarrow Si^{4+}$, $N^{3-} \rightarrow O^{2-}$) on Phase Transformation and Luminescence Properties of

$Ba_3Si_6O_{15}:Eu^{2+}$ Phosphors, *Chem. Mater*, 2017, **29**(4), 1813-1829.

4. J. Chen, N. Zhang, C. Guo, F. Pan, X. Zhou, H. Suo, X. Zhao and E. M. Goldys, Site-Dependent Luminescence and Thermal Stability of Eu^{2+} Doped Fluorophosphate toward White LEDs for Plant Growth, *ACS Appl Mater Interfaces*, 2016, **8**(32), 20856-20864.
5. X. Sheng, P. Dai, Z. Sun and D. Wen, Site-Selective Occupation of Eu^{2+} Activators Toward Full-Visible-Spectrum Emission in Well-Designed Borophosphate Phosphors, *Chem. Eng. J*, 2020, **395**, 125141.
6. X. Zhang, Z. Zhu, Z. Guo, Z. Sun, Z. Yang, T. Zhang, J. Zhang, Z.-c. Wu and Z. Wang, Dopant Preferential Site Occupation and High Efficiency White Emission in $K_2BaCa(PO_4)_2:Eu^{2+}$, Mn^{2+} Phosphors for High Quality White LED Applications, *Inorg. Chem. Front*, 2019, **6**(5), 1289-1298.
7. Y. Wang, T. Seto, K. Ishigaki, Y. Uwatoko, G. Xiao, B. Zou, G. Li, Z. Tang, Z. Li and Y. Wang, Pressure-Driven Eu^{2+}-Doped $BaLi_2Al_2Si_2N_6$: A New Color Tunable Narrow-Band Emission Phosphor for Spectroscopy and Pressure Sensor Applications, *Adv. Funct. Mater*, 2020, **30**(34), 2001384.
8. B. F. Zheng, X. T . Zhang, D. Zhang, F. K. Wang, Z. B. Zheng, X. Y. Yang, Q. Yang, Y. H. Song, B. Zou and H. F. Zou, Ultra-Wideband Phosphor $Mg_2Gd_8(SiO_4)_6O_2:Ce^{3+}$, Mn^{2+}: Energy Transfer and

Pressure-Driven Color Tuning for Potential Applications in LEDs and Pressure Sensors, *Chem. Eng. J*, 2022, **427**, 131897.

9. Z. B. Zheng, Y. Song, B. F. Zheng, Y. Zhao, Q. Wang, X. Zhang, B. Zou and H. F. Zou, *Inorg. Chem. Front*, 2023, **10**, 2788-2798.

10. Z. B. Zheng, Z. Li, H. F. Zou, Q. Tao, Y. Zhao, Q. Wang, Z. Shi, Y. Song and L. Li, Eu^{2+} and Mn^{2+} Co-Doped $Lu_2Mg_2Al_2Si_2O_{12}$ Phosphors for High Sensitivity and Multi-Mode Optical Pressure Seneing, *Inorg Chem*, 2024, **63**(9), 3882-3892.

11. T. Zheng, M. Sójka, P. Woźny, I. R. Martín, V. Lavín, E. Zych, S. Lis, P. Du, L. Luo and M. Runowski, Supersensitive Ratiometric Thermometry and Manometry Based on Dual-Emitting Centers in Eu^{2+}/Sm^{2+}-Doped Strontium Tetraborate Phosphors, *Adv. Opt. Mater*, 2022, **10**(20), 2201055.

12. K. Su, L. Mei, Q. Guo, P. Shuai, Y. Wang, Y. Liu, Y. Jin, Z. Peng, B. Zou and L. Liao, Multi-Mode Optical Manometry Based on $Li_4SrCa(SiO_4)_2:Eu^{2+}$ Phosphors, *Adv. Funct. Mater*, 2023, **33**(49), 2305359.

13. M. Szymczak, M.Runowski, M. G. Brik and L. Marciniak, Super-Sensitive Luminescent Manometer Based on Giant Pressure-Induced Spectral Shift of Cr^{3+} in the NIR Range, *Chem. Eng. J*, 2023, **466**, 143130.

14. M. Szymczak, P. Woźny, M. Runowski, M. Pieprz, V. Lavín and L.

Marciniak, Temperature Invariant Ratiometric Luminescence Manometer Based on Cr^{3+} Ions Emission, *Chem. Eng. J*, 2023, **453**, 139632.

15. M. Szymczak, M. Runowski, V. Lavín and L. Marciniak, Highly Pressure-Sensitive, Temperature Independent Luminescence Ratiometric Manometer Based on $MgO:Cr^{3+}$ Nanoparticles, *Laser Photonics Rev*, 2023, **17**(4), 2200801.

16. Y. Zhuo, F. Wu, Y. Niu, Y. Wang, Q. zhang, Y. Teng, H. Dong, Z. Mu, Super Broadband Emission Across NIR-I and NIR-II Under Blue Light Excitation of Cr^{3+}, Ni^{2+} Co-Doped Sr_2GaTaO_6 Phosphor Achieved by Two-Site Occupation and Effective Energy Transfer, *Laser Photonics Rev*, 2024, **18**(8), 2400105.